JOURNAL OF SOLID STATE CHEMISTRY **136,** 56–62 (1998)
ARTICLE NO. SC977654

MgV_2O_5 and $\delta Li_xV_2O_5$: A Comparative Structural Investigation

Patrice Millet,*,[1] Christine Satto,* Philippe Sciau,*,† and Jean Galy*

* *Centre d'Elaboration de Matériaux et d'Etudes Structurales, CNRS, 29 rue Jeanne Marvig, B.P. 4347, 31055 Toulouse Cedex, France; and † Laboratoire de Chimie Physique du Solide, Ecole Centrale de Paris, F-92295 Chatenay Malabry Cedex, France*
E-mail: millet@cemes.fr

Received May 29, 1997; in revised form October 6, 1997; accepted October 9, 1997

The structures of MgV_2O_5 and δLiV_2O_5 have been determined form X-ray powder diffraction Rietveld analysis at 294 and 83 K. The compounds crystallize in the orthorhombic system, space group *Cmcm*, with the following cell parameters (Å): at 294 K, $a_{Mg} = 3.6913(2)$, $b_{Mg} = 9.9710(4)$, $c_{Mg} = 11.0173(4)$, $a_{Li} = 3.6047(2)$, $b_{Li} = 9.9157(5)$, $c_{Li} = 11.2479(4)$; at 83 K, $a_{Mg} = 3.6928(2)$, $b_{Mg} = 9.9576(3)$, $c_{Mg} = 11.0096(4)$, $a_{Li} = 3.6031(2)$, $b_{Li} = 9.8734(4)$, $c_{Li} = 11.2350(4)$. The general network, with four formulas per unit, is built up by parallel puckered $[V_2O_5]_n$ layers of $[VO_5]$ square pyramids sharing edges and corners alternately shifted by $a/2$ in the [100] direction and held together by intercalated Mg or Li atoms. The main difference between the two is induced by the higher polarization of the magnesium atoms compared to the lithium atoms, which leads to higher puckering angles of 21.0° and 11.3°, respectively. Both magnesium and lithium atoms are surrounded by four close oxygens making a distorted tetrahedron. Despite the presence of both V^{4+} and V^{5+} in δLiV_2O_5, no electronic localization occurs at the crystallographic sites corresponding to these vanadium species. This fact could be attributed to the low energy available to the system during the low-temperature synthesis.

INTRODUCTION

Vanadium in its +V and +IV valences exhibits a remarkable oxygen coordination versatility: *CN* 4 tetrahedron (only for V^{5+}), *CN* 5 trigonal bipyramid and its continuous distortion up to square pyramid, and *CN* 6 octahedron. The intercalation or insertion of alkali, alkaline earth, or other metals into the vanadium pentoxide (V_2O_5) network has given a diverse family of nonstoichiometric $M_xV_2O_5$ compounds, i.e., the vanadium oxide bronzes (VOB), showing various structure types characterized by three-dimensional or layered networks, which have been classified by Galy (1). In the $(V_2O_5)_n$ network, vanadium exhibits the mixed valences +V and +IV. There also exist other VOB families with formulas $Li_{1+x}V_3O_8$(2), β(and β') $Li_xV_9O_{22}$, and β(and β') $Li_xV_{12}O_{29}$ (3, 4), the last of these being deduced from β(and β') $Li_xV_2O_5$ by a mechanism of double nonstoichiometry (5).

In the $Li_xV_2O_5$ VOBs Galy *et al.* (6) found four phases at 650°C, namely α, β, β', and γ. The homogeneity range of $\gamma Li_xV_2O_5$ was found to be $0.88 \leq x \leq 1$ and the structure showed puckered $[V_2O_5]_n$ layers in which, for the first time, the electronic localization was established by implying the presence of two square pyramids (SP) of widely different size (7)—$[V^{5+}O_5]$ and $[V^{4+}O_5]$—the smaller one being attributed to vanadium(V). In the $Na_xV_2O_5$ VOBs (8), among others, an orthorhombic phase, α', was isolated for $0.7 \leq x \leq 1$, and its structure was determined (9) and later refined (10). The structure of the limiting case NaV_2O_5 is roughly identical with the foliated V_2O_5 structure, the sodium lying between the $[V_2O_5]_n$ layers. The most striking point is induced by the strong electronic localization, which transforms the *Pmmn* space group (all the vanadium sites identical in V_2O_5) into the noncentric space group $P2_1mn$. Therefore two independent crystallographic sites were proposed for the $\alpha'NaV^{5+}V^{4+}O_5$ formula and, as in $\gamma Li_xV_2O_5$, two $[V_2O_5]$ SP of different size clearly established. An inverse confirmation of such localization was achieved by the structural determination in the series of the original fluoroxide bronzes $Na_xV_2O_{5-y}F_y$ for $x = y = 1$, i.e., $\alpha'NaV_2O_4F$ (11). This compound has the $\alpha'NaV_2O_5$ structural organization but vanadium is only in the +IV oxidation state and therefore the space group becomes again *Pmmn* as for V_2O_5. This was also confirmed by the synthesis of the isostructural compound CaV_2O_5, the $n = 2$ member of the series CaV_nO_{2n+1}, for which such a hypothesis (space group *Pmmn*) was formulated by Bouloux *et al.* (12), recently established by Marrot (13) by X-ray powder pattern Rietveld analysis, and determined in detail by Onoda *et al.* (14) on a single crystal.

[1] To whom correspondence should be addressed.

0022-4596/98 $25.00

Making $Li_xV_2O_5$ at room temperature, Cava *et al.* (15) found three phases, α, ε and δ. This system was thoroughly reinvestigated by Rozier *et al.* (16), who showed that the homogeneity range of the ε phase is in fact divided into two phases, ε_1 and ε_2, both with lithium intercalating a V_2O_5 type structure and with orthorhombic and monoclinic cell settings, respectively. The $\delta Li_xV_2O_5$ structure determined from powder pattern neutron diffraction showed a new structure with single $[V_2O_5]_n$ layers alternately displaced $a/2$ along the [100] direction. The corresponding V_2O_5 b parameter is then doubled and the space group becomes *Cmcm* (with $Cmc2_1$ and $C2cm$ as other possibilities). As noted by Galy (1), the cell parameters as well as the space group were almost identical with those of MgV_2O_5. The magnesium–vanadium(IV) compounds $MgVO_3$ and MgV_2O_5 were synthesized and characterized by Bouloux *et al.* (17) and the structure of $MgVO_3$ was determined. $\delta Li_xV_2O_5$ space group *Cmcm* implies that all the vanadium atoms are located on one crystallographic site and therefore there is no localization for the V^{5+} and V^{4+}. MgV_2O_5 contains only V^{4+} and should have the centric space group *Cmcm*.

To make a comparison of the phases $\delta Li_xV_2O_5$ and MgV_2O_5 similar to the one done for $\alpha'NaV_2O_5$, CaV_2O_5, and NaV_2O_4F, we have performed X-ray powder pattern Rietveld analysis of both MgV_2O_5 and δLiV_2O_5, whose structures are reported and compared herein.

TABLE 1
Data Collection, Crystal Data, and Conditions and Refinement Details

Data collection

Diffractometer: Microcontrol — Monochromator: Graphite
Instrument geometry: Bragg–Brentano — Radiation type: Cu$K\alpha$
Wavelength (Å) 1.5406 and 1.5443
2θ step/time step: 0.01°/10 s 15–40° (2θ); 0.02°/40 s 40–60° (2θ)
0.02°/80 s 60–90° (2θ); 0.05°/120 s 90–150° (2θ)

Crystal data

Crystal system: orthorhombic — Space group: *Cmcm* (No. 63) — $Z = 4$

	MgV_2O_5		δLiV_2O_5	
Parameters	294 K	83 K	294 K	83 K
a(Å)	3.6913(2)	3.6928(2)	3.6047(2)	3.6031(2)
b(Å)	9.9710(4)	9.9576(3)	9.9157(5)	9.8734(4)
c(Å)	11.0173(4)	11.0096(4)	11.2479(4)	11.2350(4)
D_x(Mg m^{-3})	3.376		3.121	
θ range (deg)	7.5–75	7.5–75	7.5–70	7.5–70

Refinement

Refinement on R_{wp} — (fwhm)$^2 = u\tan^2\theta + v\tan\theta + w$
Weighting scheme: $w = 1/\sigma^2(I)$ — Analytical function for profile:
Computer program: XND (Bérar) — pseudo-Voigt

EXPERIMENTAL

Materials Preparation

MgV_2O_5 was synthesized by solid-state reaction from a stoichiometric mixture of MgO (puriss p.a., Fluka AG) and VO_2. VO_2 was prepared by heating an equimolar mixture of V_2O_5 and V_2O_3 at 850°C under vacuum for 1 day. V_2O_3 itself was obtained by reducing V_2O_5 (99.9%, Aldrich Chemical Co.) under hydrogen at 800°C. After grinding, MgO and VO_2 were placed in a gold container

TABLE 2
Final Atomic Parameters and Agreement Factors versus Temperature for MV_2O_5 (M = Mg, Li)

	294 K		83 K	
	MgV_2O_5	LiV_2O_5	MgV_2O_5	LiV_2O_5
M				
x	$\frac{1}{2}$	$\frac{1}{2}$	$\frac{1}{2}$	$\frac{1}{2}$
y	0.3878(3)	0.3992(18)	0.3866(3)	0.3992(1)
z	$\frac{1}{4}$	$\frac{1}{4}$	$\frac{1}{4}$	$\frac{1}{4}$
B_{iso}	0.26(6)	2.53(43)	0.08(6)	0.95(33)
V				
x	0	0	0	0
y	0.2017(2)	0.2057(2)	0.2012(2)	0.2058(1)
z	0.4034(2)	0.3987(2)	0.4034(2)	0.3988(1)
B_{eq}	0.52(8)	1.93(14)	0.35(7)	1.44(10)
O1				
x	0	0	0	0
y	0.0424(4)	0.0471(4)	0.0417(4)	0.0456(4)
z	0.3727(4)	0.3728(4)	0.3725(4)	0.3732(4)
B_{iso}	0.30(13)	2.28(12)	0.76(9)	1.58(11)
O2				
x	0	0	0	0
y	0.2372(4)	0.2449(4)	0.2363(4)	0.2439(4)
z	0.5787(5)	0.5745(4)	0.5783(5)	0.5732(4)
B_{iso}	0.64(9)	2.13(15)	0.48(9)	1.25(12)
O3				
x	0	0	0	0
y	0.3044(7)	0.2808(6)	0.3035(7)	0.2864(6)
z	$\frac{1}{4}$	$\frac{1}{4}$	$\frac{1}{4}$	$\frac{1}{4}$
B_{iso}	0.56(10)	1.54(16)	0.46(10)	1.12(13)
$B_{eq} = \frac{4}{3}\sum_i\sum_j B_{ij}a_ia_j$				
Atom V				
B_{11}	0.0122(12)	0.0398(22)	0.0057(11)	0.0294(19)
B_{22}	0.0008(2)	0.0067(3)	0.0006(1)	0.0047(2)
B_{33}	0.0013(2)	0.0021(2)	0.0010(2)	0.0019(1)
B_{23}	0.0002(3)	0.0019(4)	− 0.0001(3)	− 0.0009(3)
R_{wp}(%)[a]	9.8	7.8	9.0	7.3
$R_{wp\text{-}e}$(%)	20.0	20.0	15.3	19.1
R_{Bragg}(%)	4.9	4.0	4.7	4.5
R_{exp}(%)	4.9	3.3	5.8	3.2

[a] See Table 3 for definitions of R factors.

and sealed under vacuum in a quartz tube. The mixture was then heated at 800°C for 12 hr.

δLiV_2O_5 was prepared by soft chemistry following the procedure previously described by Murphy *et al.* (20). V_2O_5 was reduced with appropriate amounts of lithium iodide in acetonitrile according to the equation

$$LiI + V_2O_5 \xrightarrow{CH_3CN} LiV_2O_5 + \tfrac{1}{2} I_2$$

The resulting mixture was stirred for 24 hr at room temperature under argon. The supernatant solution rapidly developed a dark brown color, characteristic of an acetonitrile solution of I_2. The color changed from orange to dark blue. The compound was isolated by filtration, washed under argon with acetonitrile and acetone, dried for 24 hr, and stored under argon. The lithium and vanadium contents were finally determined by elemental chemical analysis, confirming the LiV_2O_5 formula.

X-Ray Analysis

X-ray powder patterns were collected up to $\theta_{max} = 75°$ on a high-accuracy Microcontrol diffractometer, using Cu$K\alpha$ radiation (graphite monochromator) from a rotating-anode 18-kW generator (18). The angles were measured accurately by means of incremental (10^{-4}°) photoelectric encoders. The records (294 and 83 K) were performed in a flowing cryostat (stability of 0.5 K). Data collection conditions were optimized to improve the peak to background ratio. They are summarized in Table 1.

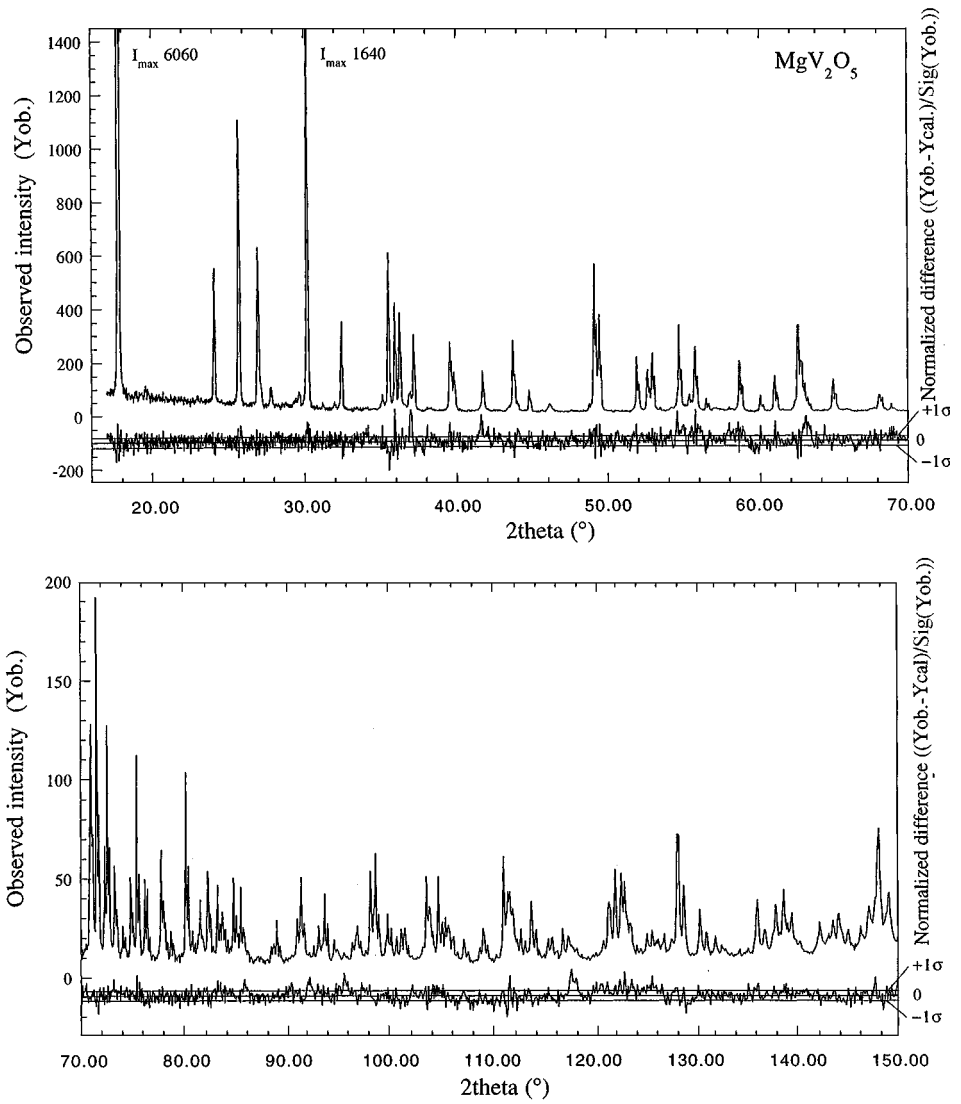

FIG. 1. Observed and difference X-ray powder patterns of MgV_2O_5. The normalized difference profile scale, indicated by the solid lines, corresponds to $\pm 1\sigma$.

Structural refinements were carried out using the Rietveld profile method by means of the XND computer program (19). Neutral-atom scattering factors were taken from the "International Tables for X-Ray Crystallography" (1974, Vol. IV). For both compounds a preferred orientation correction was used in the [010] direction.

STRUCTURE DESCRIPTION

The X-ray diffraction patterns of both compounds indicated that the phases were quite pure. Observed *d*-spacings matched those previously reported for δLiV_2O_5 and MgV_2O_5 (15, 17). Initially, the centrosymmetric space group *Cmcm* was tested and atomic parameters of δLiV_2O_5 from a neutron diffraction study (17) were used as starting values for the refinement of both structures. Final atomic parameters, cell parameters, and agreement factors for δLiV_2O_5 and MgV_2O_5 at different temperatures are listed in Table 2. Only vanadium atoms were described by anisotropic thermal parameters. Interestingly, the δLiV_2O_5 structure is more agitated as indicated by the relatively high values of the atomic thermal parameters at 294 and 83 K. The *b* parameter corresponding to the stacking of the V_2O_5 layers is the most affected by the temperature decrease whereas *a* and *c* do not vary significantly. The observed and difference profiles are plotted in Fig. 1 for MgV_2O_5 and in Fig. 2 for δLiV_2O_5. As can be seen, the profile fits are excellent, taking into account that the profile scale corresponds to $\pm 1\sigma$. Attempts to test the noncentrosymmetric space groups $Cmc2_1$ and *C*2*cm* did not give significant results (see

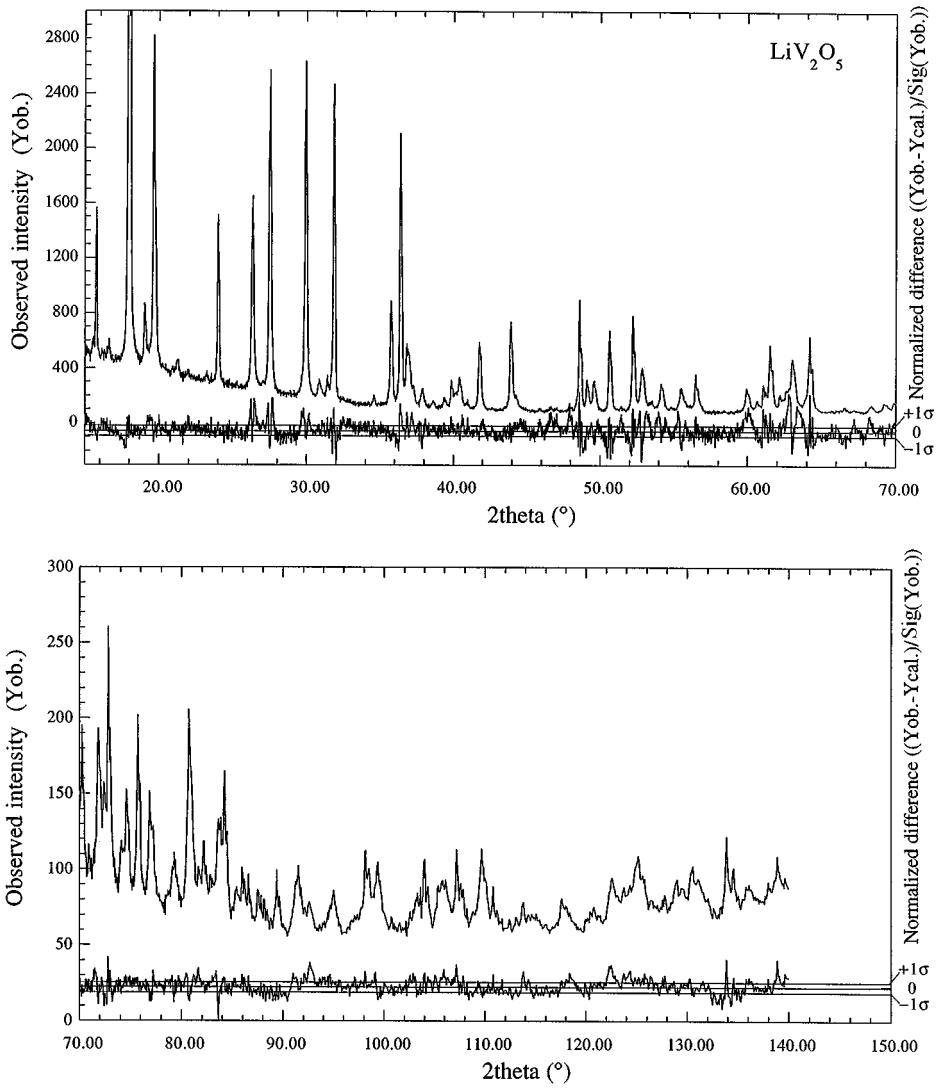

FIG. 2. Observed and difference X-ray powder patterns of δLiV_2O_5. The normalized difference profile scale corresponds to $\pm 1\sigma$.

TABLE 3
Comparison of Agreement Factors for Different Space Groups for MV_2O_5[a]

	MgV_2O_5 (83 K)		δLiV_2O_5 (83 K)		
	Cmcm	$Cmc2_1$	*Cmcm*	$Cmc2_1$	*C2cm*
R_{wp} (%)	8.98	8.87	7.33	7.37	7.43
$R_{wp\text{-}c}$ (%)	15.26	14.47	19.20	19.20	19.48
R_{Bragg} (%)	4.65	4.47	4.48	4.62	4.74
R_{exp} (%)	5.80	5.80	3.20	3.20	3.20
P	54	58	45	49	45

[a] $R_{wp} = [\sum w(Y_{o_i} - Y_{c_i})^2/\sum w(Y_{o_i})^2]^{1/2}$; $R_{wp\text{-}c}$ = modified R_{wp} taking into account the local correlations (21); $R_{Bragg} = \sum(I_o - I_c)/\sum(I_o)$; $R_{exp} = [(N_{obs} - P)/\sum(wY_o)^2]^{1/2}$, with N_{obs} the number of observations and *P* the number of refined parameters.

Table 3). For δLiV_2O_5 the number of parameters increased without improvement of the *R* factors, whereas for MgV_2O_5 the noncentrosymmetric space group $Cmc2_1$ led to slightly better *R* values but had to be rejected on the basis of crystal chemistry consideration. All vanadiums are in the +IV valence state and there is no reason to lose the mirror plane.

DISCUSSION AND CONCLUSION

As already known, the structure retains the basic frame of the V_2O_5 foliated host lattice which is built up in one direction by infinite double strings of $[VO_5]$ SP (Fig. 3) that share edges and corners along the short parameter *a* (~3.7 Å) and that are held together by corner sharing in the [001] direction (oxygen O3). This atom plays a stamp hinge role in defining the puckering of the layer measured by the dihedral angle μ (Fig. 4). Both compounds are isostructural and an idealized view of the crystal structure down the *a* axis is presented in Fig. 4. Selected interatomic distances of both structures are listed in Table 4. The insertion of Li and Mg into the V_2O_5 network results in a shift of *a*/2 along [100] for alternate layers (doubling of the short interlayer parameter) and puckering of the V_2O_5 layers to accommodate both cations. As expected, the charge difference between Mg and Li makes the former more polarizing than the latter. This is highlighted by the decrease of the *c* parameter and the puckering of the μ angle, 21.0° for MgV_2O_5 to 11.3° for δLiV_2O_5. The same evolution has been observed for the series of isostructural compounds $\alpha'NaV_2O_5$ and CaV_2O_5 (see Table 5). Li and Mg are located

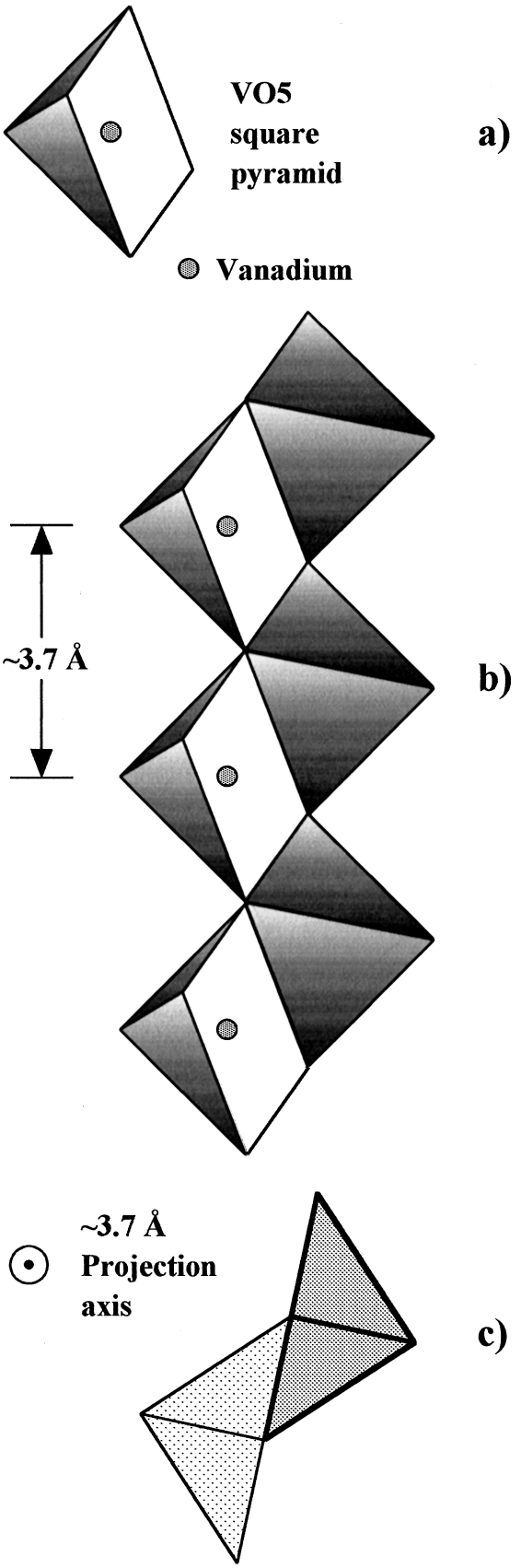

FIG. 3. Endless strings (b) of VO_5 square pyramids (a) sharing edges and corners; (c) ideal representation in projection along the short 3.7 Å parameter.

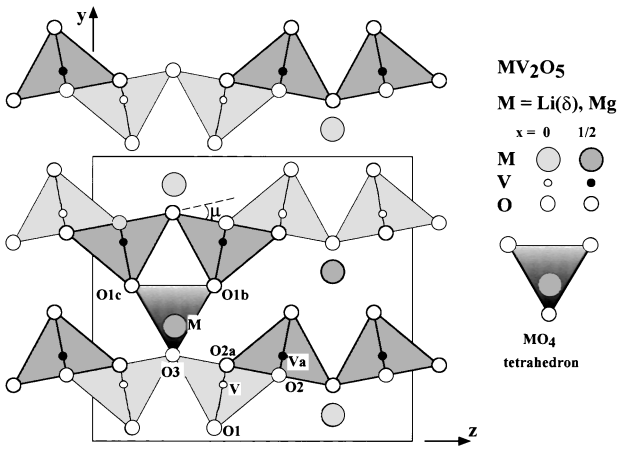

FIG. 4. Idealized structure of MV_2O_5 (M = Li, Mg) viewed down the a axis (3.7 Å) .

between the layers and surrounded by six oxygen atoms at distances ranging from 2.014 to 2.436 Å (two O2a bicapping the tetrahedron MO1cO1bO3) but only the closest four are considered to be involved in the basic bonding making a distorted tetrahedron (Fig. 5).

Vanadium in both structures is located in a SP. The strong covalent bond between vanadium and the oxygen atom O1 at the apex of the SP (typical of the vanadyl group VO^{2+}) leads to a pulling of the vanadium out of the basal plane ($d_\perp$). It is worth mentioning the differences between the mean values of the vanadium–oxygen bonding ($\langle$V–O$\rangle$) and the $d_\perp$ in both structures: $\langle V^{4+}\text{–}O\rangle_{Mg} = 1.894$ Å and $\langle V^{5+}, V^{4+}\text{–}O\rangle_{Li} = 1.846$ Å; $d_{\perp Mg} = 0.666$ Å and $d_{\perp Li} = 0.548$ Å. The $\langle V^{4+}\text{–}O\rangle_{Mg}$ and $d_{\perp Mg}$ are in excellent agreement with the values noted in other structures such as CaV_2O_5 or for the V^{4+} clearly identified in a single crystallographic site in vanadium bronzes such as γLiV_2O_5 or $\alpha'NaV_2O_5$ (see Table 5). We note that in δLiV_2O_5 the VO_5 square pyramid characteristics do not fit with the foregoing values or with the $[V^{5+}O_5]$ SP but both $\langle V^{5+}, V^{4+}\text{–}O\rangle_{Li} = 1.846$ Å and $d_{\perp Li} = 0.548$ Å are average values between pure $[V^{5+}O_5]$ and $[V^{4+}O_5]$ SP. This remark agrees well with the fact that both V^{5+} and V^{4+} coexist on the same crystallographic sites and that this careful structural determination settles the problem of electronic localization which does not occur in δLiV_2O_5 but which does occur in γLiV_2O_5 and $\alpha'NaV_2O_5$, with direct influences on space group and magnetic properties.

TABLE 4
Selected Interatomic Distances (Å) in MV_2O_5 (M = Mg, Li) at 294 K[a]

	MgV_2O_5	δLiV_2O_5
V–O1	1.624(5)	1.599(5)
–O2	1.962(6)	2.015(6)
–O2a (× 2)	1.954(2)	1.892(2)
–O3	1.975(4)	1.831(4)
$\langle$V–O$\rangle$	1.894	1.846
M–O1b	2.050(6)	2.014(14)
–O1c	2.050(6)	2.014(14)
–O2a (× 2)	2.261(5)	2.436(12)
–O3 (× 2)	2.026(3)	2.151(10)
V–Va	2.976(3)	3.035(4)

[a] Symmetry operators: a, $\frac{1}{2}+x, \frac{1}{2}-y, 1-z$; b, $\frac{1}{2}+x, \frac{1}{2}+y, z$; c, $\frac{1}{2}-x, \frac{1}{2}+y, \frac{1}{2}-z$.

TABLE 5
Vanadium–Oxygen Distances of the Square Pyramid Basal Plane ($d_\perp$) and Puckering Angles (μ) of Some Selected MV_2O_5 Phases

Phase	$\langle$V–O$\rangle$(Å)	$d_\perp$(Å)	μ (deg)	Space group	Reference
V_2O_5	1.823	V^{5+}, 0.470	0.1	*Pmmn*	(22)
γLiV_2O_5	1.876	V^{4+}, 0.636	62.0	*Pnma*	(6)
	1.826	V^{5+}, 0.539			
δLiV_2O_5	1.846	(V^{5+}, V^{4+}), 0.548	11.3	*Cmcm*	This work
MgV_2O_5	1.894	V^{4+}, 0.666 …	21.0	*Cmcm*	This work
$\alpha'NaV_2O_5$	1.889	V^{4+}, 0.698	3.2	$P2_1mn$	(10)
	1.803	V^{5+}, 0.397			
CaV_2O_5	1.886	V^{4+}, 0.648 …	11.8	*Pmmn*	(14)

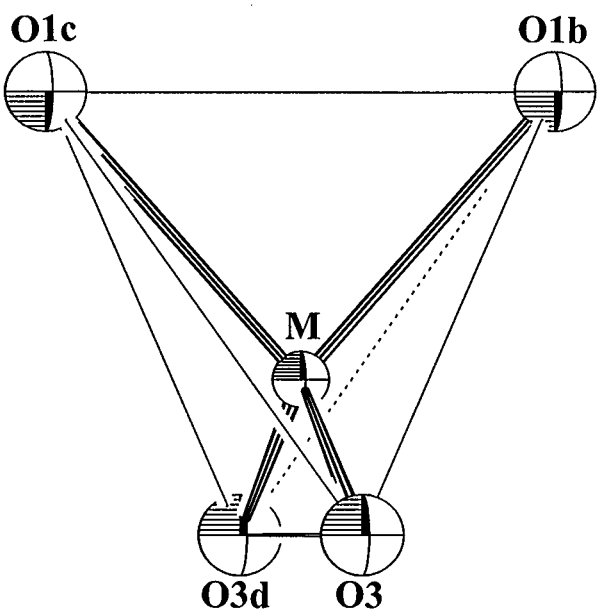

FIG. 5. Mg (or Li)–oxygen coordination polyhedra in MV_2O_5. Symmetry code (d) $1+x, y, z$.

These remarks urge us to pursue studies on this fundamental problem dealing with the electronic localization in mixed-valence compounds and particularly on the structural evolution of the δLiV_2O_5 phase, which transforms into εLiV_2O_5 after gentle heating. This latter phase exhibits a structural network similar to that of $\alpha' NaV_2O_5$, CaV_2O_5 or NaV_2O_4F, with again the ambiguity of space group $P2_1mn$ or $Pmmn$, and the α' phase corresponds to a crystallographic order between V^{5+} and V^{4+}. The end phase of this structural evolution versus temperature is γLiV_2O_5, in which V^{5+} and V^{4+} sites have been well identified. It would be interesting to follow influence of the thermal activation on the electronic localization and therefore its influence on the magnetic properties.

REFERENCES

1. J. Galy, *J. Solid State Chem.* **100,** 229 (1992).
2. A. D. Wadsley, *Acta Crystallogr.* **10,** 261 (1957).
3. K. Kato and E. Takayama-Muromachi, *Acta Crystallogr.* **C43,** 1447 (1987).
4. K. Kato and E. Takayama-Muromachi, *Acta Crystallogr.* **C43,** 1451 (1987).
5. J. Galy, J. M. Savariault, and C. Roucau, *Aust. J. Chem.* **49,** 1009 (1996).
6. J. Galy, J. Darriet, and P. Hagenmuller, *Rev. Chim. Miner.* **8,** 509 (1971).
7. J. Galy and A. Hardy, *Acta Crystallogr.* **19,** 432 (1965).
8. A. Hardy, J. Galy, A. Casalot, and M. Pouchard, *Bull. Soc. Chim. Fr.* **4,** 1056 (1965).
9. J. Galy, A. Casalot, M. Pouchard, and P. Hagenmuller, *C. R. Acad. Sci.* **262,** 1055 (1966).
10. J. Galy and A. Carpy, *Acta Crystallogr.* **B31,** 1481 (1985).
11. A. Carpy and J. Galy, *Bull. Soc. Fr. Miner. Cristallogr.* **94,** 24 (1971).
12. J. C. Bouloux and J. Galy, *J. Solid State Chem.* **16,** 385 (1976).
13. J. Marrot, Thesis, Université Paul Sabatier, Toulouse, 1995.
14. M. Onoda and N. Nishiguchi, *J. Solid State Chem.* **127,** 359 (1996).
15. R. J. Cava, A. Santoro, D. W. Murphy, S. M. Zahurak, R. M. Fleming, P. Marsh, and R. S. Roth, *J. Solid State Chem.* **65,** 63 (1986).
16. P. Rozier, J. M. Savariault, J. Galy, C. Marichal, J. Hirschinger, and P. Granger, *Eur. J. Solid State Inorg. Chem.* **t.33,** 1 (1996).
17. J. C. Bouloux, I. Milosevic, and J. Galy, *J. Solid State Chem.* **16,** 393 (1976).
18. J. F. Bérar, G. Calvarin, and D. Weigel, *J. Appl. Crystallogr.* **13,** 201 (1980).
19. J. F. Bérar and P. Garnier, APD 2nd Conference, N.I.S.T Special Pub. **846,** 212 (1992).
20. D. W. Murphy, P. A. Christian, F. J. Disalvo, and J. W. Wazczak, *Inorg. Chem.* **18,** 2800 (1979).
21. J. F. Bérar and P. Lelann, *J. Appl. Crystallogr.* **24,** 1 (1991).
22. R. Enjalbert and J. Galy, *Acta Crystallogr.* **C42,** 1467 (1986).